Journal of Intelligent Manufacturing, 14, 219–228, 2003

Estimation of shrinkage for near net-shape using a neural network approach

ABDULLAH KONAK,[1] SADAN KULTUREL-KONAK,[1]
ALICE E. SMITH[2] and IAN NETTLESHIP[3]

[1]*Penn State Berks-Lehigh Valley College, Reading, PA 17610 USA*
E-mail: konak@psu.edu, sadan@psu.edu
[2]*Department of Industrial and Systems Engineering, Auburn University, Auburn, AL 36849 USA*
E-mail: aesmith@eng.auburn.edu
[3]*Department of Materials Science and Engineering, University of Pittsburgh, Pittsburgh, PA 15261 USA*
E-mail: nettles@engrng.pitt.edu

Received June 2001 and accepted December 2001

A neural network approach is presented for the estimation of shrinkage during a hot isostatic pressing (HIP) process of nickel-based superalloys for near net-shape manufacture. For the HIP process, the change in shape must be estimated accurately; otherwise, the finished piece will need excessive machining and expensive nickel-based alloy powder will be wasted (if shrinkage is overestimated) or the part will be scrapped (if shrinkage is underestimated). Estimating shape change has been a very difficult task in the powder metallurgy industry and approaches range from rules of thumb to sophisticated finite element models. However, the industry still lacks a reliable and general way to accurately estimate final shape. This paper demonstrates that the neural network approach is promising to estimate post-HIP dimensions from a combination of pre-HIP dimensions, powder characteristics and processing information. Compared to nonlinear regression models to estimate shrinkage, the neural network models perform very well. Furthermore, the models described in this paper can be used to find good HIP process settings, such as temperature and pressure, which can reduce operating costs.

Keywords: Hot isostatic pressing (HIP), artificial neural networks, powder metallurgy, near net-shape

1. Introduction

Hot isostatic pressing (HIP) is a chipless metal-working process to make parts with excellent creep life, fatigue resistance, durability and strength by consolidating metal, ceramic or composite powders under pressure and temperature. As capacity and capability of HIP equipment improved over the last two decades, the number and range of parts manufactured by the HIP process have dramatically increased (Atkinson and Rickinson, 1991). The popularity of the HIP process can be attributed to its capability of producing near net-shape parts in various shapes and dimensions with homogenous microstructures. The HIP process is used to produce high-quality and high-performance superalloy parts made from a mixture of nickel, iron, chromium and cobalt.

Superalloys can maintain their stability and strength at elevated temperatures and are increasingly used in aerospace, medical, defense and energy products that operate in severe environments (Wilson *et al*., 1996). The complex chemistry of superalloys limits the application of traditional ingot casting due to severe macroscopic segregation. More uniform microstructures, free from macrosegregation, can be achieved by the HIP process, therefore, it is the preferred manufacturing process for superalloy parts. A major problem of the HIP process is to estimate the anisotropic shrinkage of the powder geometry and shape deformation during powder consolidation.

Achieving dimensional control is extremely difficult for large parts, even for simple shapes such as solid cylinders with large length-to-diameter ratios. An accurate and comprehensive model of the HIP process will enable cost-effective production of parts by reducing post-HIP machining and scrap.

Neural networks (NNs) have been successfully applied to model many complex manufacturing processes (see e.g., Coit *et al*., 1998; Cook and Chiu, 1998; Kyeong *et al*., 2000; Sathyanarayanan *et al*., 1992; Smith, 1993) where there is no satisfactory analytical model or where simpler models, such as linear or quadratic, are inappropriate. Katz and Naude (1999) employ NNs to model the relationship between the features of a part and process parameters and outcome for electro discharge machining. Raj *et al*. (2000) showed the effectiveness of NN models in a metal forming manufacturing system that includes hot extrusion, and metal cutting. Schlang *et al*. (1996) discuss how NN models are used in Siemens to estimate the process variables of electric arc furnaces and hot rolling mills. Two comprehensive surveys on the subject are (Udo, 1992; Zhang and Huang, 1995). This paper presents an NN based method to predict the shrinkage and shape distortion for nickel-based superalloy solid cylinders manufactured by the HIP process. The NN combines pre-HIP shape dimensions, processing parameters and characteristics of the superalloy powder to accurately estimate post-HIP dimensions. This project is wholly based on industrial production data and was accomplished through the partnership with a leading manufacturer of superalloy products for the aircraft, power and medical industries.

2. Background

2.1. *Powder metallurgy and hot isostatic pressing*

In the powder metallurgy (P/M) process, parts are made by compacting metal powders using high pressure and/or temperature. Although P/M has grown in popularity in recent decades, it is one of the oldest manufacturing technologies known to man to make metal tools and jewelry, tracing its history to 3000 BC (German, 1984). The P/M process consists of three main steps: (1) powder production, (2) blending/screening and (3) powder compaction.

Metal powder can be produced by any of several techniques such as atomization, reduction, electrolytic deposition, commination and mechanical alloying (Kalpakjian, 1995). The objective of the blending/screening operation is to obtain a homogenous powder mass with a uniform particle size distribution, which is essential for good compaction. In the compaction step, the powder is transformed into hard parts by applying pressure. Initially, the powder is not fully dense due to voids between particles, however as pressure increases, porosity decreases due to (first) better arrangement and (later) plastic deformation of the powder particles (German, 1984). By applying sufficient pressure, voids collapse and the powder is consolidated to full theoretical density. Isostatic pressing, where pressure is uniformly applied from all directions (isostatic) in order to achieve uniform compaction, has become widely accepted as an effective method for compaction. HIP is the application of pressure (approximately 15,000 psi) at temperatures usually greater than 70% of the melting temperature of the material (Atkinson and Rickinson, 1991). Since pressure is applied uniformly, relatively large compacts can be produced with uniform density and strength, which is difficult to achieve using other compaction techniques.

Figure 1 shows the basic steps of the HIP process: (i) loading, (ii) outgassing, (iii) HIP and (iv) removal of the exterior container. In the HIP process, a steel container, which is engineered to compensate for the shrinkage during compaction, is filled with metal powder. During loading, the container is vibrated to reduce porosity and achieve uniform powder packing. The loaded powder is approximately 70% dense. In the outgassing step, residual gases are pumped out as the container is heated. In the compaction step, pressure and heat are simultaneously applied until the powder is consolidated to full theoretical density and becomes a solid part. As a result, the initial

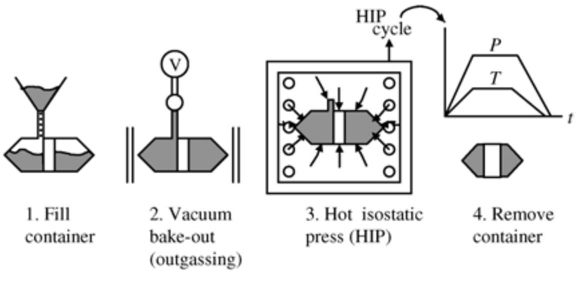

Fig. 1. Steps of the HIP process.

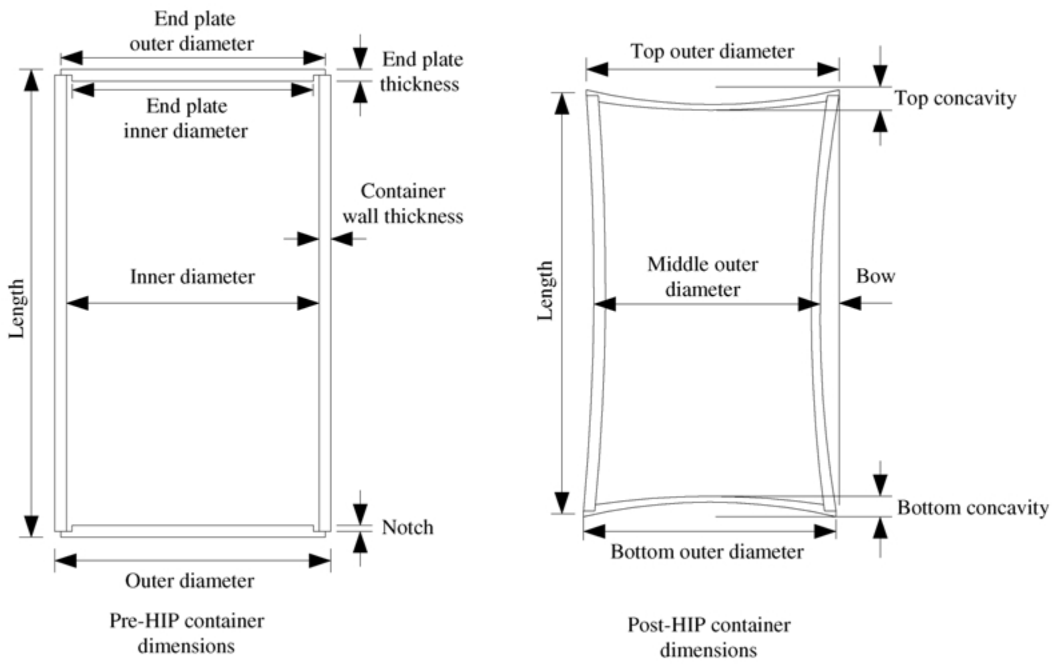

Fig. 2. Shrinkage and shape distortion of solid cylinders during the HIP process.

dimensions of the container are reduced by 5–15% (Nissen *et al*., 1989). Ideally, the shrinkage of the container is expected to be uniform in every dimension (isotropic shrinkage) since the pressure is applied uniformly. However, actual shrinkage deviates from ideal isotropic shrinkage because of imperfections in the process. Finally, the exterior container is removed, leaving the near net-shape.

2.2. *Motivation for the project*

The P/M and the HIP processes are costly manufacturing processes, requiring large investment and specialized production skills and they are used to produce high consequence components for the medical, aerospace and mining industries. One important advantage of the HIP process is that parts are produced at or near net-shape, eliminating the need for secondary machining and reducing scrap of expensive superalloys. More than 97% of the starting raw material is used in the final part (MPIF, 2001). However, to fully achieve the benefits of near net-shape, the shrinkage during the HIP process must be estimated accurately. If shrinkage is overestimated, additional machining will be required and expensive powder will be wasted. If it is underestimated, the part may be scrapped. Shrinkage is difficult to estimate because parts do not shrink uniformly and shape distortions may occur due to the structural design of containers and/or the filling uniformity of the powder. This anisotropic shrinkage and shape distortion, as shown in Fig. 2 for solid cylinders (a commonly manufactured shape), may cause final compacts to deviate from targeted dimensions. A model to estimate the shrinkage of a given container will help engineers to design the containers such that the final compact is close to the targeted dimensions, minimizing the need for additional machining and the chance of scrapping.

Furthermore, there are opportunities for cost reduction of the HIP process itself. To achieve full densification, containers are exposed to pressure and elevated temperatures for extended time periods. After compacts reach full density, continuation of pressure has little benefit (German, 1984). Therefore, optimizing the HIP cycle in terms of temperature and pressure over time can provide operational cost saving.

2.3. *Existing approaches for HIP process modeling*

Traditionally, containers are designed by trial-and-error, which requires considerable time and money to achieve a good container design. It was recently reported that costs associated with this approach can exceed $750,000 (NCEMT, 2001). If isotropic shrinkage is assumed, relative linear shrinkage (S) for a solid cylinder can be given as follows (Nissen *et al.*, 1989):

$$S = \left(\frac{V_C + V_P \times \rho}{V_C + V_P} \right)^{1/3}$$

where V_C is the volume of the container; V_P the volume of the powder and ρ the packing ratio (ratio of packing density of powder to theoretical density).

Given the initial diameter of a container (OD_i), its final diameter (OD_f) can be estimated by $OD_f = OD_i \times S$. Garibov *et al.* (1979) showed that the isotropic model is a good approximation for solid cylinders with diameter to height ratios of between 1 to 2. In an experimental study, Nissen *et al.* (1989) found that the following factors caused actual shrinkage to deviate from the isotropic model:

- packing density and variations in powder density
- relative container thickness and aspect ratio (length/diameter)
- pressure and heating rate during the HIP cycle
- position of container welds
- material parameters of the powder and container.

Considering these factors Nissen *et al.* (1989) developed an empirical model to predict post-HIP dimensions of solid/hollow cylindrical and rectangular shape containers with between 0.6–1.0% dimensional accuracy. This model is essentially an empirical adjustment of the isotrophic shrinking model. First, the local powder density is computed by integrating a weight function over different regions of the container. Then, the isotropic shrinkage model is used to estimate the shrinkage of different regions of the container. Finally, the isotropic estimations are corrected to include the influence of aspect ratio of the container. The correction parameters and the weight functions are determined by a least squares fit to a data set. Olevkys *et al.* (1998) suggested a mathematical method to control anisotropic shrinkage by manipulating the thickness of the container wall and the end plates. These two models represent a macroscopic approach, where the compact is assumed to be a continuous medium. The other approach is microscopic, where the HIP process is modeled by analyzing the behavior of individual particles and porosity (Atkinson and Davies, 2000). Microscopic models, e.g., that defined by Delo *et al.* (2000), mainly focus on the influence of the microstructural properties of the powder particles and the process parameters on plastic deformation and densification. Finite element analysis (FEA), which can simulate the complex relationship between the process and powder parameters, has emerged as a powerful tool to model powder compaction and the shrinkage (Khazami-Zadeh and Petzoldt, 1995; NCEMT, 2001). These models, however, are expensive to develop, and still differ in their predictions from what is experienced in industrial production.

Another direction in HIP process modeling is using soft computing. Cherian *et al.* (2000) used a NN to select powder and process parameters such as sintered density, compaction pressure, sintering temperature and sintering atmosphere. Smith and Midha (1999) proposed a rule-based expert system to evaluate the manufacturability of parts by P/M. The project herein also uses a soft computing approach, this time applied to the complicated but important task of estimating post-HIP dimensions and is the first known application of neural networks to the subject. The NN model is distinct from Nissen *et al.* (1989) in several ways. Their model does not estimate deformations (i.e., departures from a perfect shape) and does not consider HIP processing parameters. Their model does have the potential advantage of using the local packing density of powder whereas in this paper a single packing density for the entire container is used.

3. Methodology

3.1. *Data*

On advice of the industrial partner, the project focused on a specific nickel based superalloy formed in solid cylinders. Both the alloy and the shape are the most common ones manufactured by this company. A repository consisting of the relevant historical HIP data of the industrial partner was created in a relational database. Since the data came from a variety of sources, some in software form and some in paper form, compiling the data was a significant task. The data was then purified through elimination of outliers and incomplete observations. This left 200 observations to be used in model development and validation.

Definitions of the dependent and the independent variables included in the data repository are:

(i) *Pre-HIP container dimensions*:

- length
- inner and outer diameters (measured at the top and at the bottom)
- wall thickness
- inner and outer diameters of the end-plates at the top and at the bottom
- thickness of the end-plates
- notch of the end-plates

(ii) *Filling data*:

- packing ratio (PR) of the powder

(iii) *Processing data*: The original process data includes measurements of pressure and temperature inside the autoclave every minute during the HIP cycle (see Fig. 3 for a typical pressure profile; temperature follows a similar pattern). A typical HIP cycle has two plateaus, termed Dwell I and Dwell II, where pressure and temperature remain nearly steady. The minute by minute observations were condensed to:

- beginning minute of Dwell I
- beginning minute of Dwell II
- duration of Dwell I
- duration of Dwell II
- minutes between the start of Dwell I and the end of Dwell II
- average pressure (psi) during Dwell I
- average temperature (°F) during Dwell I
- average pressure (psi) during Dwell II
- average temperature (°F) during Dwell II
- pressure (psi) change from the averages of Dwell I to Dwell II

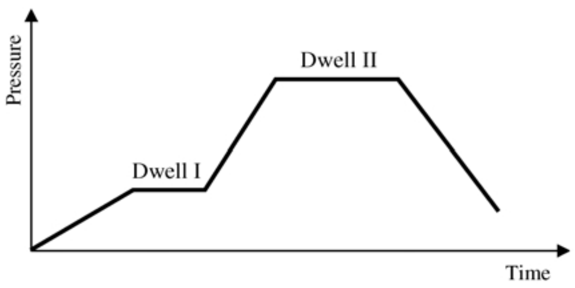

Fig. 3. Typical pattern of pressure variation during a typical HIP cycle.

- temperature (°F) change from the averages of Dwell I to Dwell II
- average pressure (psi/min) increase rate from Dwell I to Dwell II
- average temperature (°F/min) increase rate from Dwell I to Dwell II
- total applied pressure (psi/min) during a HIP cycle (calculated by numerically integrating under the pressure over time curve)
- total applied temperature (°F/min) during a HIP cycle (calculated by numerically integrating under the temperature over time curve)

(iv) *Placement*: The location of the heaters and the placement of containers may affect heat distribution within the autoclave, influencing the shape distortion. In order to indicate the location of the containers with respect to the heaters, the bottom of the autoclave is divided into two zones, central and outer.

- zone of containers (central or outer)
- distance between the bottom of a container and the base of the autoclave
- total volume of containers (inch^3) processed in a HIP cycle
- distribution of the total volume between the central and the outer zones

(v) *Post-HIP dimensions*: (to be estimated, i.e., the dependent variables):

- length
- diameter of the container measured at the top, middle and bottom
- concavity of the container's end plates at the top and bottom
- axial concavity of the container (''bow'')

3.2. *Constructing and validating the neural networks*

Seven separate NN models were constructed to predict the seven post-HIP dimensions listed above. All networks were fully connected feed-forward networks with two hidden layers and trained by a standard backpropagation-learning algorithm. This NN is known to be a universal approximator (Funahashi, 1989; Hornik *et al*., 1989), which means it should be capable of modeling any relationship regardless of form or complexity. Input and output vectors were normalized between ± 1 and the same transfer function was used in each neuron in a given

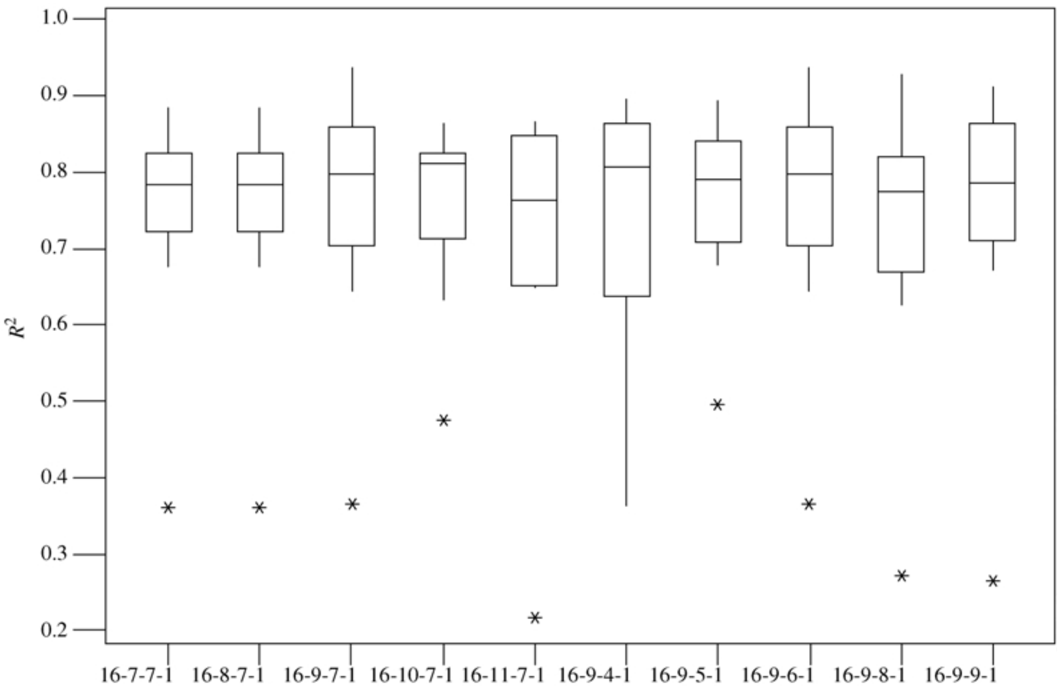

Fig. 4. Typical box plot (this one of top concavity) of coefficient of determination (R^2) for different network architectures.

NN. Network architectures were selected after preliminary experimentation assessing performance using 10 fold cross validation (Twomey and Smith, 1998). Performance was not strongly dependent on the architectures tested, however there was some effect as shown in Fig. 4. The final network architectures are presented in Table 1 where for example, 10-10-7-1 represents 10 inputs, 10 neurons in the first hidden layer, 7 neurons in the second hidden layer and a single output.

In the selection of the independent variables (input vectors) for each NN model, the relevant pre-HIP dimensions and PR were always used. Then, a stepwise regression was carried out to identify the significant process variables for each post-HIP dimension. This procedure was designed to eliminate process variables that did not contribute to the explanation of the variance of the dimension being predicted, not to test a linear relationship. If any process variable (including placement) was significant, then all process variables were included as inputs so that the model could have access to a complete description of the HIP cycle. This turned out to be the case for only the curvature measures—top and bottom concavity and bow. The specific inputs to each model are listed in Table 1.

Since this project is intended for industrial use, validating the generalization ability of the NN models was particularly important. As in choosing the network architecture, a ten-fold cross validation approach was used (Twomey and Smith, 1998). This approach, while more computationally laborious, leverages all data by using each observation for both model construction and, independently, model validation. Therefore, a validation network was trained on 180 observations and tested on the remaining 20 observations, and this process was repeated for a total of ten times, each with a different 20 observation test set. The final application network was trained by using the entire data set of 200 under identical conditions as the validation networks. Its generalization performance is inferred from the averaged test set performance of the ten validation networks.

4. Results and discussion

To form a baseline for comparison, several regression models were built and validated using the same data sets and the same ten-fold cross validation approach. Full second-order polynomial regression (with the

Table 1. The NN models for each post-HIP dimension

Variables	*NN model*						
	Length (10-10-7-1)	*Top outer diameter (8-5-4-1)*	*Middle outer diameter (8-5-4-1)*	*Bottom outer diameter (8-5-4-1)*	*Top concavity (16-9-7-1)*	*Bottom concavity (18-11-7-1)*	*Bow (17-10-7-1)*
Container outer diameter (inch)	x	x	x	x	x	x	x
Container inner diameter (inch)	x						
Container length (inch)	x				x	x	x
Container wall thickness (inch)	x	x	x	x	x	x	x
Aspect ratio (Length/Diameter)	x	x	x	x	x	x	x
End plate outer diameter (inch)	x	x	x	x	x	x	
End plate inner diameter (inch)	x	x	x	x	x	x	
End plate thickness (inch)	x	x	x	x	x	x	x
End plate notch (inch)	x	x	x	x	x	x	
Packing ratio (%)	x	x	x	x	x	x	x
Ratio of can weight to can volume (lb./inch^3)							x
Location of container (zone)					x	x	x
Start time of Dwell I (min)							x
Duration of Dwell I (min)					x	x	x
Mean pressure during Dwell I (psi)					x	x	x
Mean temperature during Dwell I (F°)					x	x	x
Duration of Dwell II (min)					x	x	x
Mean pressure during Dwell II (psi)					x	x	x
Mean temperature during Dwell II (F°)					x	x	x
Time from the start of Dwell I to the end of Dwell II (min)							x
Ramp time from Dwell I to Dwell II (min)						x	
Temperature ramp rate from Dwell I to Dwell II (F°/min)							x
Total applied pressure (min × psi)						x	

additional term of $PR^{1/3}$ added to be consistent with the isotropic shrinking model) and nonlinear (exponential) regression models were tested using a stepwise approach. Figure 5 shows the mean absolute error (MAE) and root mean squared error (RMSE) for each prediction model where the regression model was the best among the kinds tested.[1] Performance of validation regression and NN are comparable for the middle and bottom diameters while the NN is better on the other dimensions. Considering MAE, the NN model was statistically better than the regression model for the estimation of post-HIP length and top diameter at 95% confidence in a one-tailed paired *t*-test. The average MAE of the validation networks was 0.18846, providing an average 0.31% absolute precision for estimating post-HIP length, which is better than earlier reported results (Nissen *et al*., 1989). There were no statistically significant differences in the performance of the NN and the regression models for post-HIP middle and bottom diameters. This might be explained by the differences in the design of the top and bottom endplates. The top endplate has a hole that is used to fill powder into containers. After outgassing, the hole is sealed and welded, making the structural design of the top endplate different than the bottom endplate. In addition, during the loading process, the power at the bottom of the container is vibrated longer than the powder at the top, which may result in less uniform powder distribution near the top. Because of these reasons, the deviation from the isotropic shrinkage model may be greater at the top. This deviation is better handled by the NN, resulting in the statistically significant improved predictions of top diameter.

Continuing this line of reasoning, the isotropic shrinkage model does not apply to the bow nor the

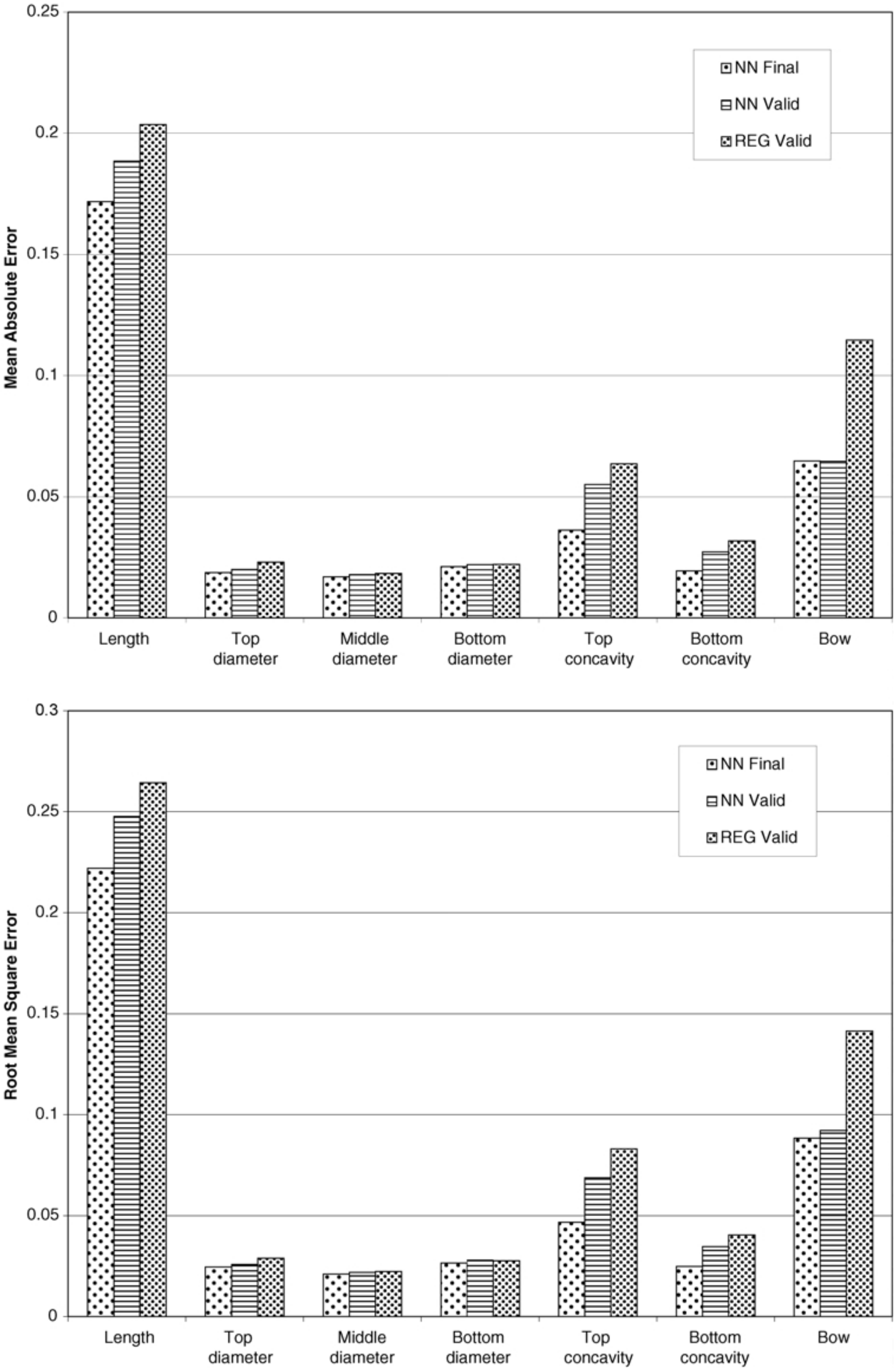

Fig. 5. Mean absolute errors and root mean square errors of models.

Table 2. Coefficient of determination (R^2) for estimates

Dimension	*Final NN*	*Validation NN*	*Validation regression*
Length	0.999	0.999	0.999
Top diameter	0.998	0.998	0.998
Middle diameter	0.999	0.999	0.999
Bottom diameter	0.998	0.998	0.998
Top concavity	0.893	0.759	0.657
Bottom concavity	0.834	0.668	0.520
Bow	0.801	0.791	0.443

concavity measures of shape distortion. The average MAEs of the validation NN were 0.05507 (12.3% accuracy) for top concavity and 0.027305 (13.3% accuracy) for bottom concavity, with the regression models' MAEs slightly more. The regression model for bow performed poorly. For bow, the averaged MAE for the validation NN was 0.06462, yielding 23.7% absolute accuracy, while the best regression MAE was 0.11460. Clearly, shape distortion prediction is much more difficult than length and diameter changes. Part of this difficulty can be attributed to human imperfections in the shape distortion measurement process where the operator must select the point of maximum difference or deformation.

Table 2 shows the coefficients of determination (R^2) of the models. It can be observed the values are not much different for the application networks and the validation networks, suggesting that the NN models have unbiased generalization and are not overtrained or overfitted, common neural network problems (Geman *et al.*, 1992).

5. Conclusions

Estimating shape change and shrinkage is always an important aspect of near net-shape manufacturing. It is also difficult to do precisely in a production environment. Previous work has concentrated on detailed FEA models or on rules of thumb. Both fall short of being effective methods for use in a plant. This paper puts forth a new method using neural networks that is shown to be accurate. Using production data that describes the pre-HIP dimensions, the powder packing ratio, the placement of the containers within the autoclave and the temperature/pressure changes over time during the cycle, predictive models were constructed and validated. While these models were specific to a common nickel-based superalloy and the solid cylindrical shape, the method would be appropriate to other alloys and other shapes. While either regression or NN models can be used for some dimensional estimations, the polynomial or exponential format of regression did not allow sufficient flexibility to model the more complicated shape distortions, most notably the bow and top cavity. Where NN and regression perform roughly equivalently, as in the middle and bottom diameters, a regression would be preferred because of the ease of model building and validating along with its statistically theoretic properties of estimation. However, when dealing with the harder estimations, the extra effort of NN models pays off in significantly improved accuracy.

The constructed models have been embedded into a user-friendly software system using a database and pull down menus. No special expertise, software or equipment is needed on the part of the user. Associated with the prediction models is a complete production database that allows the metallurgical engineers to look at trends over time and to look at short term variability in graphic formats. The industrial partner is currently using this system on a trial basis and has reported good results thus far.

Acknowledgment

This project is supported by NSF grant DMI-9800430 and by considerable in kind support by the industrial partner.

Notes

1. While length appears largest, its nominal measurement is much larger, making the relative error quite small.

References

Atkinson, H. V. and Davies, S. (2000) Fundamental aspects of hot isostatic pressing: an overview. *Metallurgical and Materials Transactions A: Physical Metallurgy and Materials Science*, **31**(12), 2981–3000.

Atkinson, H. V. and Rickinson, B. A. (1991) *Hot Isostatic Processing*, Galliard (Printers) Ltd., Norfolk, UK.

Cherian, R. P., Smith, L. N. and Midha, P. S. (2000) A neural network approach for selection of powder metallurgy materials and process parameters. *Artificial Intelligence in Engineering*, **14**, 39–44.

Coit, D. W., Jackson, B. T. and Smith, A. E. (1998) Static neural network process models: considerations and case studies. *International Journal of Production Research*, **36**(11), 2953–2967.

Cook, D. F. and Chiu, C.-C. (1998) Using radial basis function neural networks to recognize shifts in correlated manufacturing process parameters. *IIE Transactions*, **30**, 227–234.

Delo, D. P., Dutton, R. E., Semiatin, S. L. and Piehlier, H. R. (1999) Modeling of hot isostatic pressing and hot triaxial compaction of Ti–6A1–4V powder, *Acta Mater.*, **47**(11), 3159–3167.

Funahashi, K. (1989) On the approximate realization of continuous mappings by neural networks. *Neural Networks*, **2**, 183–192.

Garibov, G. S., Samarov, V. N. and Feigin, V. I. (1979) Design of capsules for the hot hydrostatic pressing of disks from heat-resisting nickel alloy powders. *Soviet Powder Metallurgy and Metal Ceramics*, **18**(2), 136–140.

Geman, S., Bienenstock, E. and Doursat, R. (1992) Neural networks and the bias/variance dilemma, *Neural Computation*, **4**, 1–58.

German, R. M. (1984) *Powder Metallurgy Science*, Metal Powder Industries Federation.

Hornik, K., Stinchcombe, M. and White, H. (1989) Multilayer feedforward networks are universal approximators. *Neural Networks*, **2**, 359–366.

Kalpakjian, S. (1995) *Manufacturing Engineering and Technology*, Addison-Wesley Publishing Company, Inc., Reading, MA.

Katz, Z. and Naude, J. (1999) A neural network/expert system approach for design improvement of products manufactured by EDM. *Transactions of the ASME, Journal of Manufacturing Science and Engineering*, **121**, 733.

Khazami-Zadeh, M. and Petzoldt, F. (1995) Hot isostatic pressing of near net shape parts through finite element simulation. *Advances in Powder Metallurgy and Particulate Materials Proceedings of the 1995 International Conference & Exhibition on Powder Metallurgy & Particulate Materials*, **2**, 5/125–5/138.

Kyeong, K. L., Brown, T., Dagnall, G., Bicknell-Tassius, R., Brown, A. and May, G. S. (2000) Using neural networks to construct models of the molecular beam epitaxy process. *IEEE Transactions on Semiconductor Manufacturing*, **13**(1), 34–45.

MPIF (2001) web site: http://www.mpif.org.

NCEMT (2001) web site: http://www.ncemt.ctc.com/modsim/hip.

Nissen, A., Jaktlund, L.-L., Tegman, R. and Garvare, T. (1989) Rapid computerized modeling of the final shape of HIPed axisymmetric containers. *Proceedings of the Second International Conference on Hot Isostatic Pressing: Theory and Applications*, pp. 55–61.

Olevsky, E., Maximenko, A., Van Dyck, S, Froyen, L., Delaey, L. and Buekenhout, L. (1998) Container influence on shrinkage under HIP-I. shrinkage anisotropy of a cylindrical specimen. *International Journal of Solids and Structures*, **35**(18), 2283–2303.

Raj, K. H., Sharma, R. S., Srivastava, S. and Patvardhan, C. (2000) Modeling of manufacturing processes with ANNs for intelligent manufacturing. *International Journal of Machine Tools and Manufacture*, **40**, 851–868.

Sathyanarayanan, G., Lin, I. J. and Chen, M.-K. (1992) Neural network modeling and multiobjective optimization of creep feed grinding of superalloys. *International Journal of Production Research*, **30**, 2421–2438.

Schlang, M., Poppe, T. and Gramchow, O. (1996) Neural networks for steel manufacturing. *IEEE Expert*, August 1996, 8–9.

Smith, A. E. (1993) Predicting product quality with backpropagation: A thermoplastic injection molding case study. *International Journal of Advanced Manufacturing Technology*, **8**, 252–257.

Smith, L. N. and Midha, P. S. (1999) A knowledge based system for optimum and concurrent design, and manufacture by powder metallurgy technology. *International Journal of Production Research*, **37**(1), 125–137.

Twomey, J. M. and Smith A. E. (1998) Bias and variance of validation methods for function approximation neural networks under conditions of sparse data. *IEEE Transactions on Systems, Man, and Cybernetics*, Part C, **28**, 417–430.

Udo, G. J. (1992) Neural network applications in manufacturing processes. *Computers and Industrial Engineering*, **23**, 97–100.

Wilson, R. K., Flower, H. L., Hack, G. A. J. and Isobe, S. (1996) Nickel-base alloys for severe environments. *Advanced Materials & Processes*, **3**, 19–22.

Zhang, H.-C. and Huang, S. H. (1995) Applications of neural networks in manufacturing: A state-of-the-art survey. *International Journal of Production Research*, **33**, 705–728.